Satellight
Commission of the European Communities

DNMI
Det norske meteorologiske institutt

Second SATELLIGHT meeting, Bergen June 24 - 25 1996

RETROSPECTIVE QUALITY CONTROL OF SOLAR RADIATION DATA

by

Jan Asle Olseth, Arvid Skartveit, and Endre Skaar

SATELLIGHT Programme JOR3-CT950041
First draft, June 1996

1. INTRODUCTION

Quality control of solar radiation data includes measures taken prior to sensor deployment in the field (sensor calibration/characterization), real time automatic quality control tests during measurement, and retrospective data analysis. Some quality control criteria may rely on redundancy in the observed data, like for instance the requirement that global irradiance equals the sum of diffuse plus beam irradiance. In the absence of such redundancy, some retrospective quality control is possible by identification of data which may be adequately tested against reliable models. The present note focuses on some aspects of retrospective quality control applied to solar radiation data from Norway.

2. DATA

Hourly global radiation measured by CM11 pyranometers are available from the following 13 stations: Bergen (University of Bergen), Gävle (Royal Institute of Technology), Ås (Norwegian Agricultural University), and 10 stations (Apelsvoll, Kise (CM5), Løken, Landvik, Særheim, Furuneset, Kvithamar, Tromsø, Tjøtta, Vågønes) run by the Norwegian Crop Research Institute.

3. THE CLEARNESS INDEX

The clearness index k for a given period is most commonly obtained by dividing the observed global irradiation H by the extraterrestrial global irradiation. In the present note, we instead choose to divide by an "average" cloud-free irradiation H_o:

$$k = H/H_o \, . \qquad (1)$$

H_o is computed from a broad-band model [1] which accounts for Rayleigh scattering, water vapour absorption, ozone absorption, aerosol scattering, aerosol absorption, and multiple reflection between the surface and the sky dome. The corresponding model inputs are station altitude, precipitable water vapour, columnal ozone, broad-band single scattering albedo 0.75, turbidity derived from an average latitudinal covariation between turbidity and precipitable water vapour [2], and surface albedo. It is stressed that, in the present note, the monthly input data estimated for Bergen (except station elevation) are used at all stations.

3.1 The frequency distribution of hourly clearness index

The frequency distribution of observed hourly clearness index was formed within three solar elevation intervals for each station and year. The choice of clearness index bins of width 0.01 demonstrates that these distributions in our climate have a narrow mode close to unit clearness index. Even though cloud traces and even variations in pressure/ozone/humidity/turbidity/albedo certainly contribute to widen this mode, its rather conspicuous narrowness obviously derives from cases of cloudless/nearly cloudless sky. In our climate, clouds affect clearness index more than does any other factor. Clouds may either block the sun and thus reduce the clearness index substantially below unity, or they may raise the clearness index significantly beyond unity when they enhance the diffuse irradiance more than they reduce the beam irradiance. Due to differences in cloud climatology, the percentage of hours within this "cloudless" mode may therefore certainly vary substantially between stations, but to some degree the mode index itself provides some quality control "fingerprint" related to model vs observation consistency under cloudless sky.

An example of how these distributions may help in malfunction diagnosis, is seen by comparing the two neighbouring stations Kise and Apelsvoll. Scatter diagrams (Fig. 1) show a high correlation between daily clearness indices from these two stations, but from 1993 to 1994 the bulk of Apelsvoll indices shift significantly upward relative to the bulk of Kise indices. Furthermore, while the hourly clearness index distributions at Kise 1993 and Apelsvoll 1993/1994 all have narrow modes close to unity, the Kise 1994 mode is shifted significantly downward (Figs. 2a-b). These hourly frequency distributions

thus strongly indicate that the daily scatter diagram shift from 1993 to 1994 (Fig. 1) is due to some as yet unresolved malfunction at Kise during 1994.

Fig. 3 show the observed hourly clearness index frequency distribution for 12 stations during 1995. For example, the significant frequency of clearness indices > 1.5 at solar elevation 10 - 20° at Løken (Fig. 3a) proved to be a spring phenomenon, most probably caused by the neglection of highly reflective snow cover at this alpine station.

3.2 The spatial distribution of mode clearness index

An exact mode index was determined from a quadratic curve through the three bin centres having the maximum frequency when summed within three consecutive bins. The mode indices for 11 stations (21 station years, 1993/94) are summarized in Fig. 4. The mode index shifts on the average only slightly upward with decreasing solar elevation, thus indicating that the solar elevation dependency of the observations is reasonably well removed by relating the clearness index to the modelled cloud-free irradiation H_o rather than to the extraterrestrial one. The mode index varies moderately between stations, and, not unexpectedly, this variation increases with decreasing solar elevation. Løken (61.1°N, 550 m a.s.l), which is the only station above 250 m elevation, has an average mode index some 0.03 higher than the average for the northern stations (63.5 - 69.7°N), presumably due to decreasing water vapour and turbidity with increasing elevation. Presumably due to an average northward decrease of water vapour and turbidity, these northern stations in turn have an average mode index which is some 0.02 higher than the average for the southern stations (58.3 - 61.3°N) below 250 m elevation. Despite quite pronounced cloudiness differences, no mode index differences between east or west of the mountain range are seen among these southern stations.

4. SHADE RING CORRECTION

At Aas, the hourly diffuse irradiance is measured by applying a black 5 cm wide shade ring of diameter 30.5 cm. As an example, the hourly diffuse fractions of global irradiance during 1995 are plotted prior to shade ring correction in Fig. 5a. The maximum fractions (observed under overcast sky) are close to unity during winter, when the sky fraction blocked out by the shade ring at these latitudes is small and located at low angular elevations. During summer, when the blocked sky fraction is greater and extends to higher angular elevations, the maximum diffuse fractions drop significantly below unity. The isotropic correction of Drummond [3] tends to raise the maximum diffuse fractions slightly beyond unity (Fig. 5b), while the maximum fractions obtained by the shade ring correction of Littlefair [4] are closer to unity (Fig. 5c).

5. REFERENCES

1. J.A. Davies and D.C. McKay, Estimating solar irradiance and components. Solar Energy **29**, 55 (1982).
2. A. Skartveit and J.A. Olseth, The probability density and autocorrelation of short-term global and beam irradiance. Solar Energy **49**, 477 (1992).
3. A. J. Drummond, On the measurement of sky radiation. Arch. Met. Geophys. Bioklim. **7**, 413 - 436 (1956).
4. P. J. Littlefair, Correcting for the shade ring used in diffuse daylight and radiation measurements. Pp. 233 - 241 in Proceedings of the CIE-WMO international symposium on Daylight and Solar Radiation Measurement, 9 - 11 October 1989 Berlin, Germany.

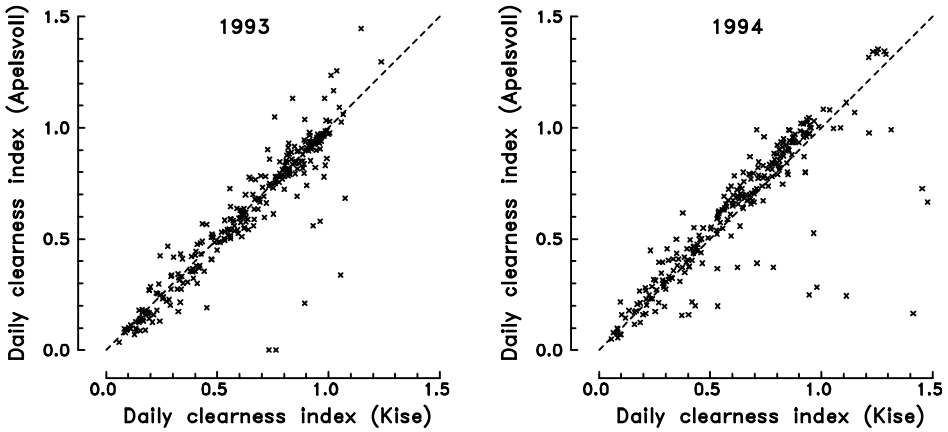

Fig.1 Two years of daily clearness indices at Apelsvoll plotted vs corresponding indices from Kise.

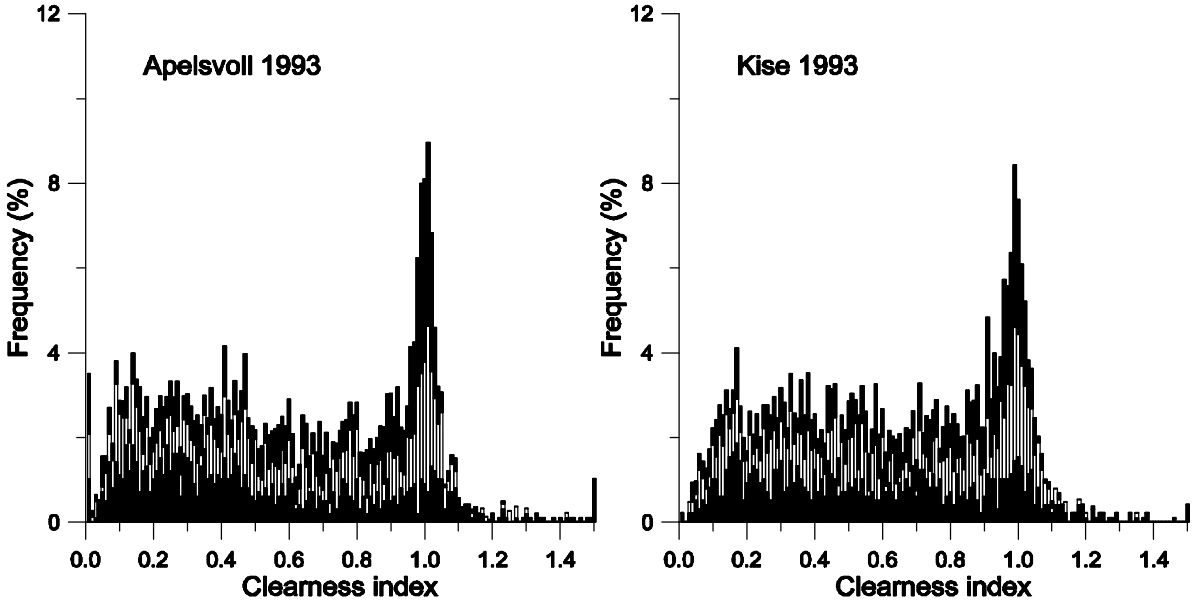

Fig.2a Distribution (percentage) of observed hourly clearness index within bins of width 0.01. Data from Apelsvoll and Kise during 1993 grouped into three solar elevation intervals: 10 - 20° (bottom), 20 - 30° (middle), and > 30° (top). See text for further details.

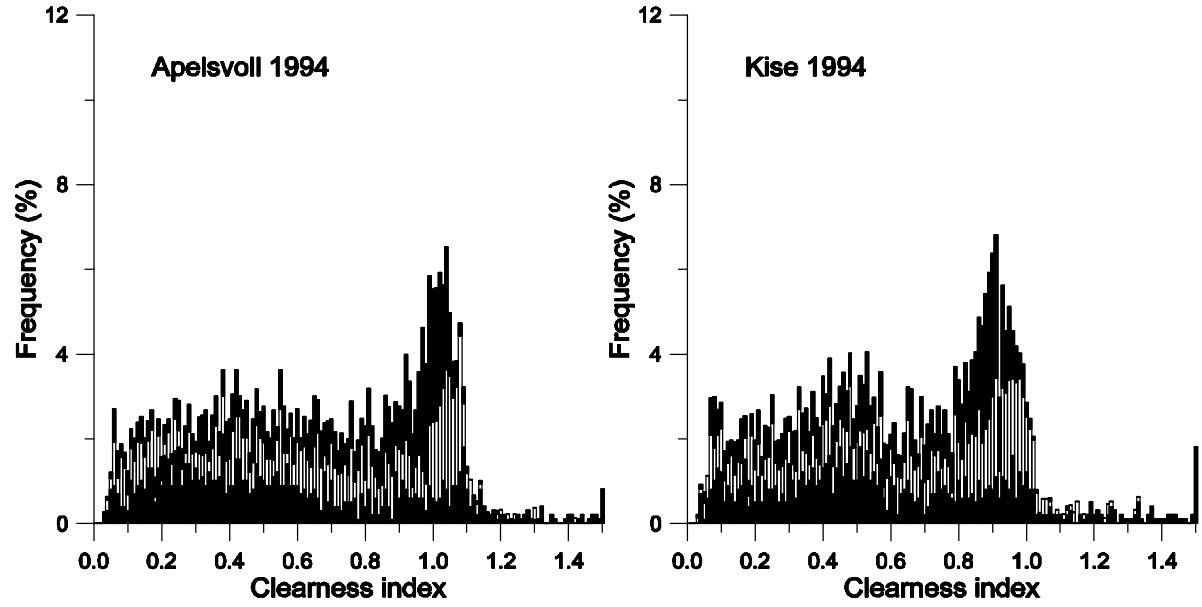

Fig.2b Same as a), but for 1994.

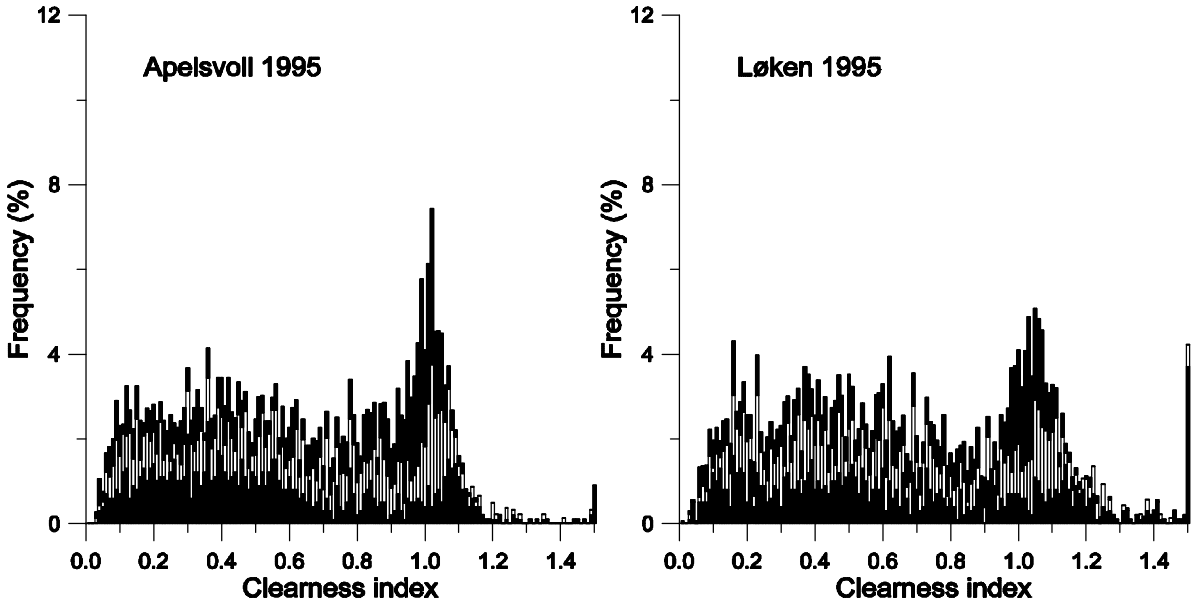

Fig.3a Same as Fig. 2a, but for Apelsvoll and Løken 1995.

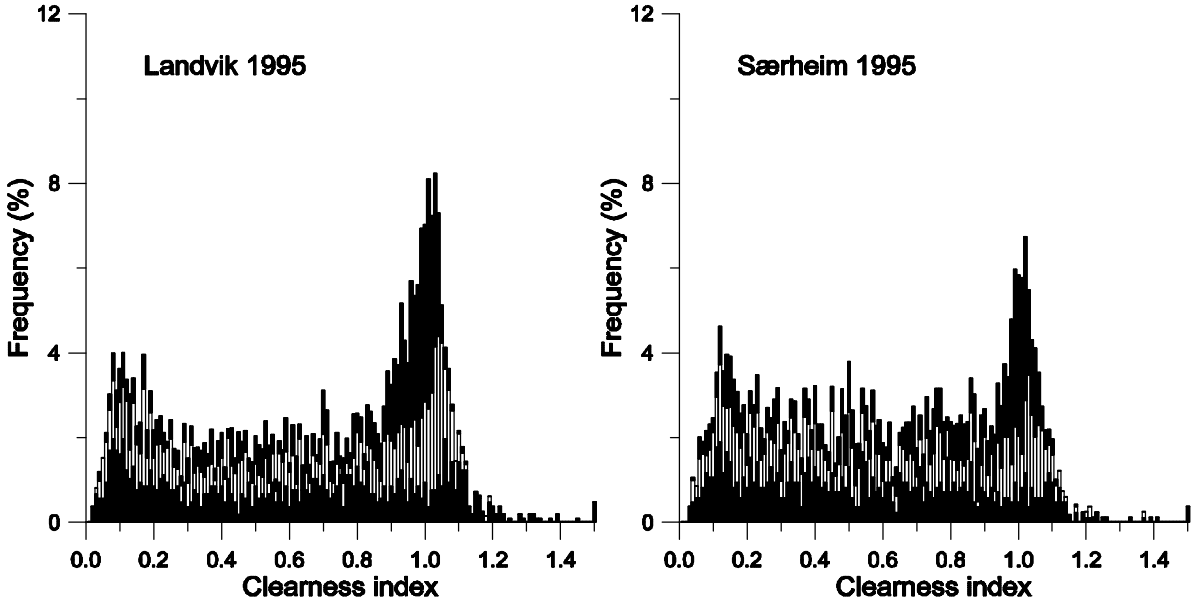

Fig.3b Same as Fig. 2a, but for Landvik and Særheim 1995.

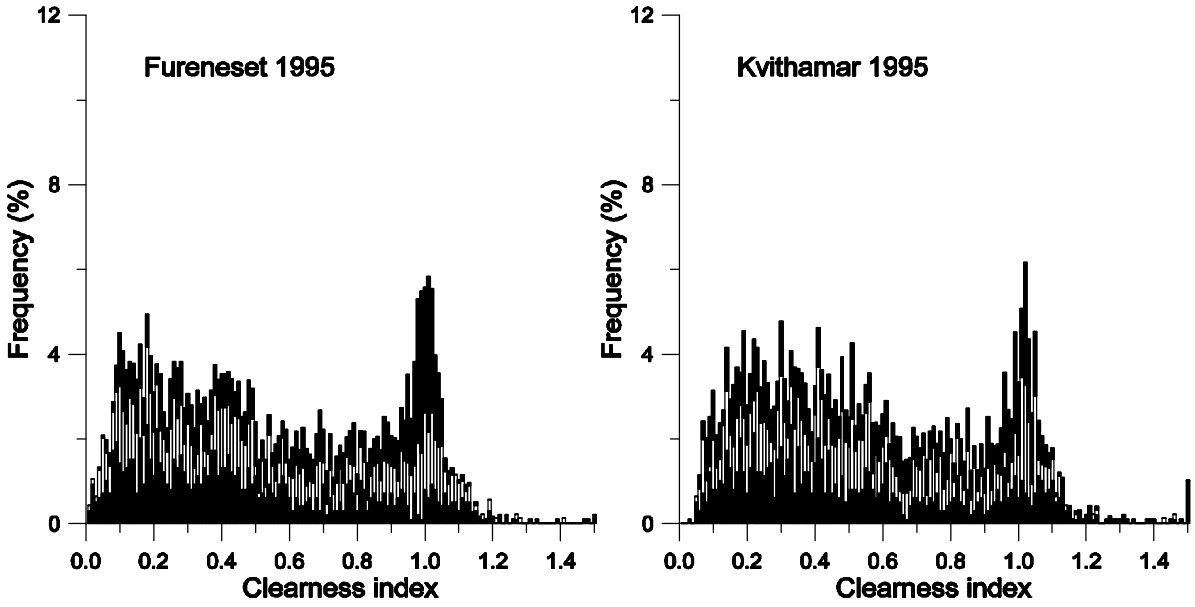

Fig.3c Same as Fig. 2a, but for Fureneset and Kvithamar 1995.

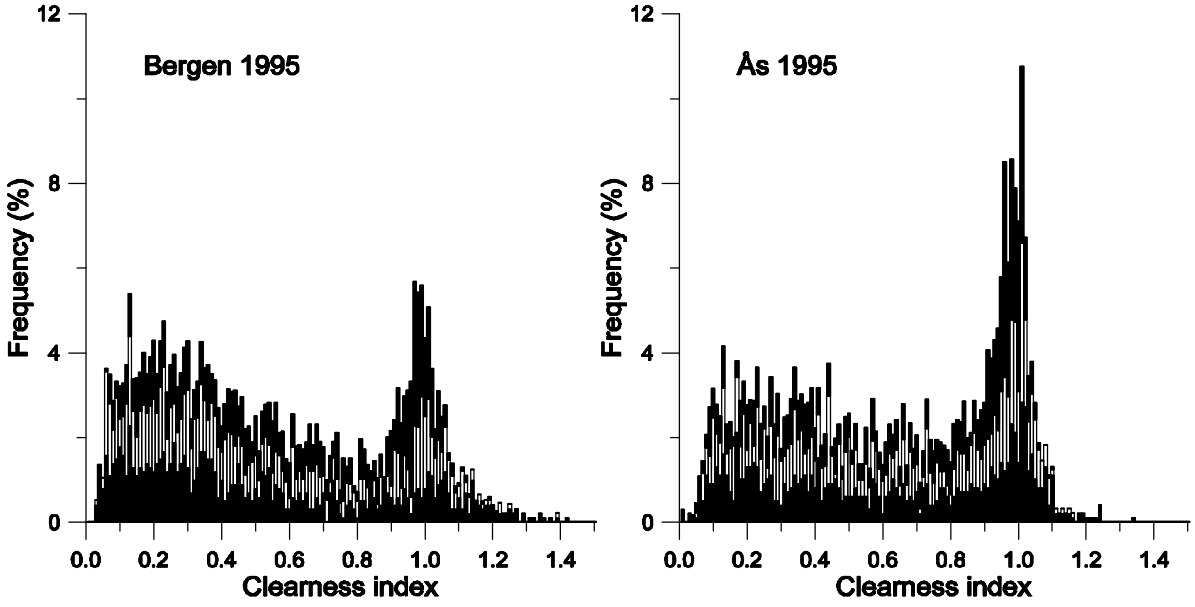

Fig.3d Same as Fig. 2a, but for Bergen and Ås 1995.

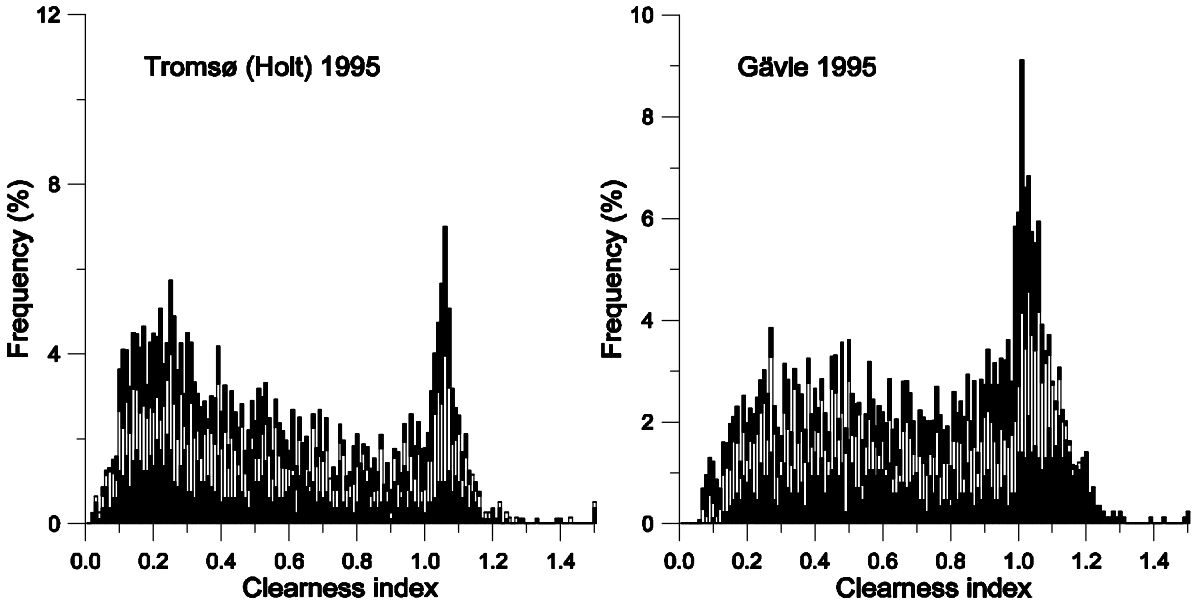

Fig.3e Same as Fig. 2a, but for Tromsø and Gävle 1995.

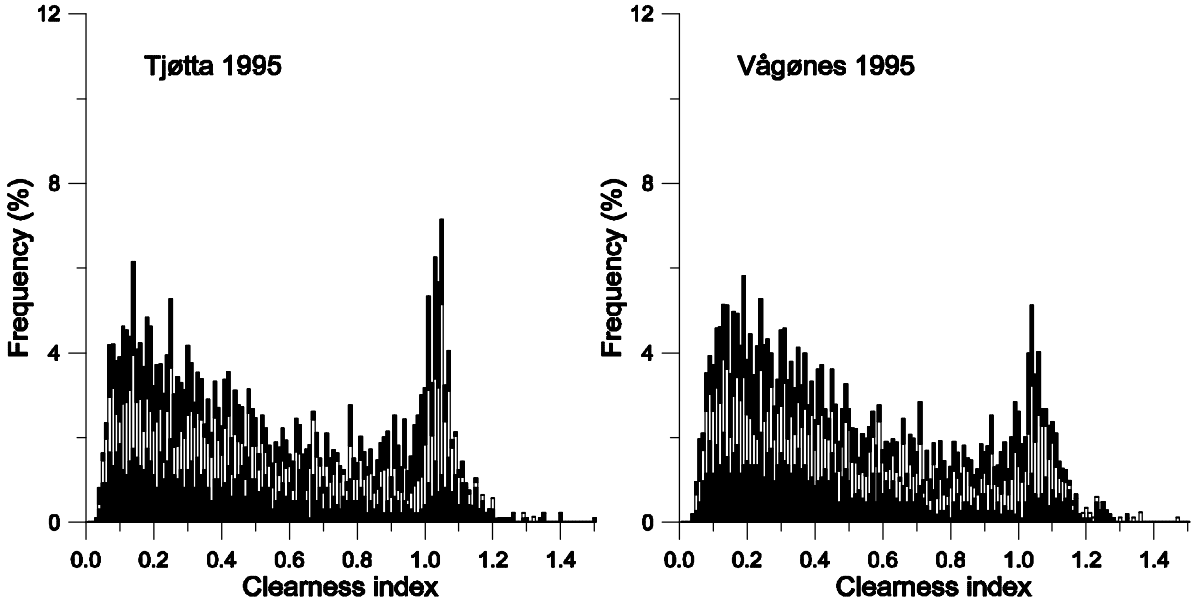

Fig.3f Same as Fig. 2a, but for Tjøtta and Vågønes 1995.

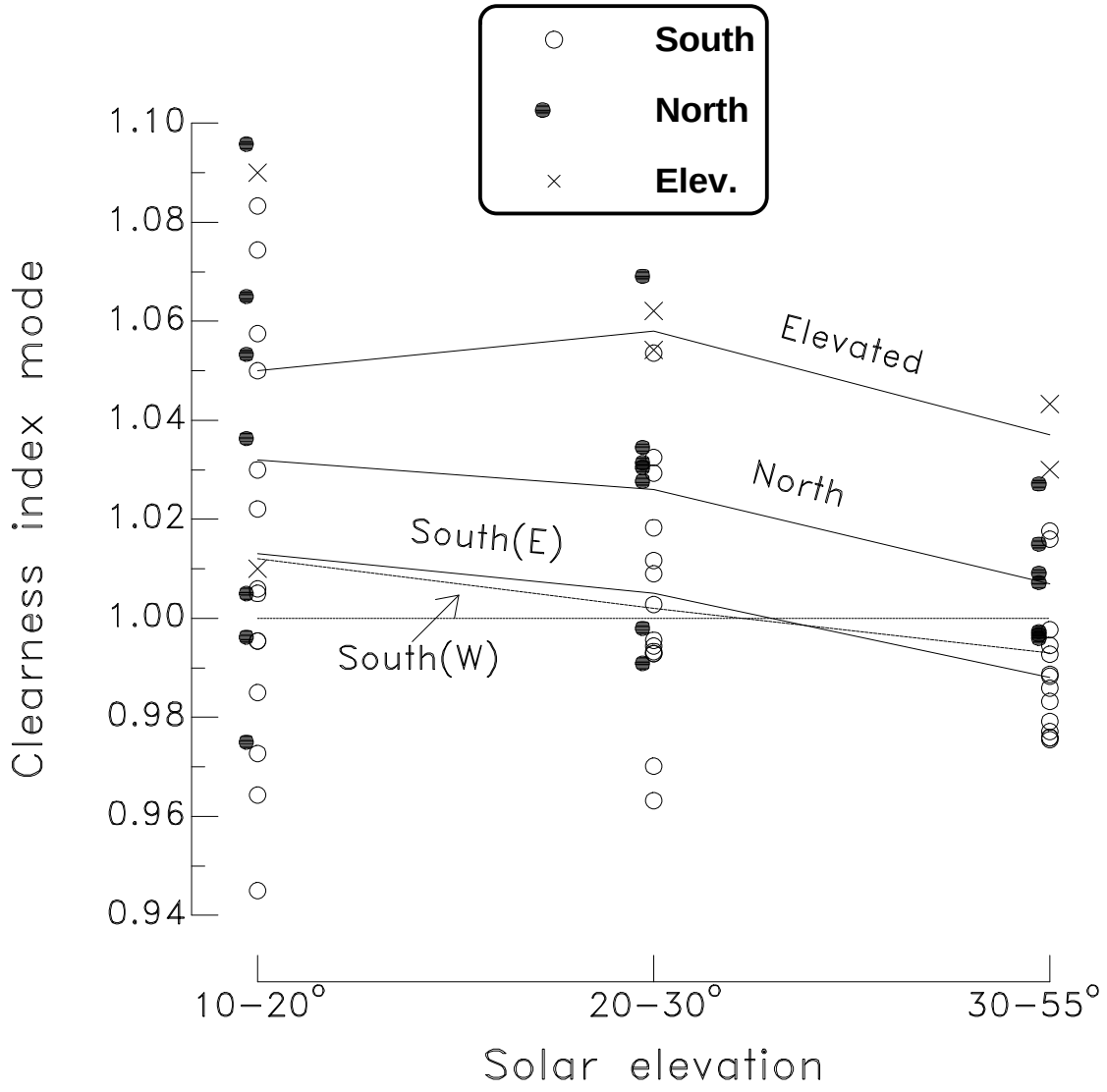

Fig.4 "Cloudless" mode indices of hourly clearness index distributions from 11 stations. Mode indices are evaluated (see text) within 3 solar elevation intervals for each one of 21 station years, 1993/94), and group mean indices are formed for the elevated station, the northern (63.5 - 69.7°N) group, and the southern (58.3 - 61.3°N) group east (E) and west (W) of the mountain chain.

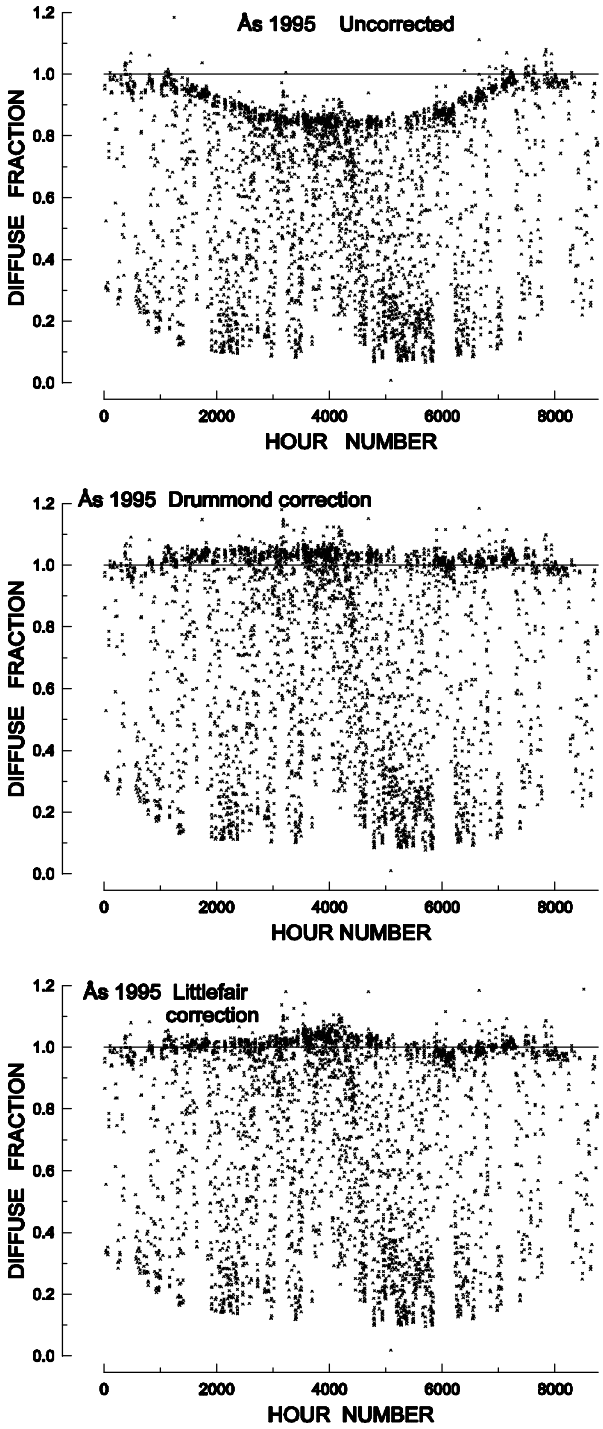

Fig.5 Top: Hourly diffuse fractions of global irradiance observed at Aas during 1995, with no shade ring correction applied.
Middle: Same as above, but with the isotropic shade ring correction of Drummond [3] applied.
Bottom: Same as above, but with the shade ring correction of Littlefair [4] applied.